NACA RM E51H08

NACA

RESEARCH MEMORANDUM

INVESTIGATION OF A 24-INCH SHOCK-IN-ROTOR TYPE

SUPERSONIC COMPRESSOR DESIGNED FOR SIMPLE

RADIAL EQUILIBRIUM BEHIND NORMAL SHOCK

By Harold Lown and Melvin J. Hartmann

Lewis Flight Propulsion Laboratory
Cleveland, Ohio

FOR REFERENCE

CLASSIFICATION CHAN...

NOT TO BE TAKEN FROM THIS ROOM

To_____ UNCLASSIFIED _____

NACA Res Abs

Authority of rRN-119 · Date Aug. 16, 1957

NATIONAL ADVISORY COMMITTEE
FOR AERONAUTICS
WASHINGTON
December 12, 1951

2266

NATIONAL ADVISORY COMMITTEE FOR AERONAUTICS

RESEARCH MEMORANDUM

INVESTIGATION OF A 24-INCH SHOCK-IN-ROTOR TYPE SUPERSONIC

COMPRESSOR DESIGNED FOR SIMPLE RADIAL EQUILIBRIUM

BEHIND NORMAL SHOCK

By Harold Lown and Melvin J. Hartmann

SUMMARY

The design of a 24-inch-diameter supersonic-compressor rotor based
on the establishment of simple radial equilibrium behind the normal
shock and a controlled diffusion rate was investigated in Freon-12.
Inlet guide vanes were used as a means of establishing the theoretically
required entrance conditions. This design followed from a previous
investigation of a 24-inch-diameter supersonic-compressor rotor.

A maximum total-pressure ratio of 2.02 at an adiabatic efficiency
of 0.74 and a weight flow of 61.5 pounds per second were obtained at an
equivalent tip speed of 1590 feet per second, with supersonic flow
existing over the entire passage height. The investigation further
revealed that although the radial accelerations behind the shock were
theoretically reduced over most of the passage, this reduction had no
apparent effect on the radial redistribution of mass flow. The shock
boundary-layer interaction pattern and associated effects must be con-
sidered along with the theoretically computed radial forces.

The shock-in-rotor type supersonic compressor offers a serious
problem in subsonic diffusion because of the shock boundary-layer inter-
action. This problem, in addition to the considerations of radial
forces, must be solved before good stage performance can be realized for
this type of compressor.

INTRODUCTION

An analytical study of supersonic axial-flow compressor performance
(reference 1) has indicated that stage pressure ratios of around 3 are
feasible for the shock-in-rotor type supersonic compressor. In order to
obtain the desired pressure ratio for this type of rotor, however, dif-
fusion of the relative Mach number at the blade exit to 0.60 or below
is required. Failure to obtain this diffusion presents one of the ser-
ious limitations on the performance of the shock-in-rotor type supersonic
compressor.

A previous investigation of a 24-inch shock-in-rotor type supersonic compressor (reference 2) revealed that the discrepancy between design pressure ratio 2.82 and the pressure ratio at design speed, 1.93, was due to incomplete passage diffusion, which in turn was due, at least partly, to the lack of simple radial equilibrium directly behind the normal shock. The necessity of approximating the condition of simple radial equilibrium after the shock was indicated. This equilibrium consideration was then incorporated in the design of this supersonic-compressor rotor investigated at the NACA Lewis laboratory.

The design theoretically reduced the diffusion problem in two manners: through the establishment of favorable conditions for diffusion by the elimination of the unbalanced radial forces behind the shock, and through the careful regulation of the subsonic passage diffusion. That a balance between the radial pressure force and the centrifugal force (simple radial equilibrium) behind the shock could be established by the proper distribution of the turning in the inlet guide vanes was assumed. An analysis of the design flow in the subsonic portion of the passage indicated that with simple radial equilibrium behind the shock and a controlled diffusion rate the resulting radial flow components were negligible.

The rotor, designed on the basis of the foregoing analysis, was investigated over the tip-speed range from 1760 to 1184 feet per second in Freon-12. Two-dimensional cascade performance of the rotor-blade pitch section, and data of the guide-vane performance, as a separate component in the compressor rig, are also included in this report.

SYMBOLS

The following symbols are used in this report:

a velocity of sound, (ft/sec)

F_r unbalanced radial force (toward the hub),

$$\frac{d(p_4/P_o)}{d(r/r_t)} - \frac{(p_4/P_o)\ \gamma V_{\theta,4}^2}{a_4^2\ r/r_t}$$

M absolute Mach number, ratio of stream velocity to local velocity of sound

M' relative Mach number, ratio of stream velocity relative to rotor to local velocity of sound

2266

P   total, or stagnation pressure, (lb/sq ft)

p   static, or stream pressure, (lb/sq ft)

r   compressor radius, (in.)

U   velocity of rotor, (ft/sec)

V   velocity of fluid, (ft/sec)

W.   weight flow, (lb/sec)

β angle between flow direction and axis, (deg)

γ ratio of specific heats

δ ratio of actual inlet total pressure to standard sea-level pres-
        sure, $P_0/2116$

η_{ad} adiabatic efficiency

θ ratio of actual inlet-stagnation temperature to standard sea-level
        temperature, $T_0/518.4$

ρ density, (lb/cu ft)

Subscripts:

o   initial stagnation conditions

2   rotor entrance

4   immediately after shock in rotor

5   rotor exit

t   tip

x   blade chord distance

z   axial component

θ tangential component

COMPRESSOR DESIGN METHOD

The design procedure was devised to determine simple radial equi-
librium behind the shock thereby eliminating the radial accelerations
that would exist in the absence of equilibrium. The method involved a
trial-and-error procedure for determining the rotor entrance flow condi-
tions based on the following assumptions: (1) the existence of simple
radial equilibrium behind the guide vanes, (2) negligible radial flow
components in the supersonic portion of the passage, and (3) the attain-
ment of the theoretical Mach number behind the shock. The entrance con-
ditions at the tip and the supersonic passage turning were fixed. From
the specified entrance conditions at the tip (rotor speed, guide-vane
turning, and absolute entrance Mach number), the flow conditions in the
minimum section were determined from the Kantrowitz contraction ratio
(reference 3), the rotor turning, and the normal shock relations. The
desired pressure behind the shock at an incremental radial distance
from the tip was evaluated by using the pressure gradient necessary for
simple radial equilibrium

$$\frac{d(p_4/P_o)}{d(r/r_t)} = \frac{(p_4/P_o) \, rV_{\theta,4}^2}{a_4^2 \, (r/r_t)}$$

and the pressure at the rotor tip. The relative entrance Mach number
that will give the required value of p_4/P_o at this lower radius was

then determined from a trial-and-error solution. The amount of guide-
vane turning depended on the relative entrance Mach number, the rotor
speed, and the absolute inlet velocity. The design method was followed
in a step-by-step manner until the rotor hub was reached. The guide-
vane turning gradient resulting from this design procedure was fairly
large (fig. 1), varying from 0° at the tip to approximately 27° at the
root. The relative entrance Mach number varied from 1.667 at the tip to
1.607 at the root.

The subsonic portion of the passage was designed to maintain a low
diffusion rate at all radii. The diffusion rate selected in this design
$\Delta(p_4/P_o)$ per inch was equal to 0.05 and corresponds approximately to a
2° equivalent cone based upon the minimum and exit areas. No contouring
of the hub or shroud was necessary in this design since the radial veloc-
ities computed at the exit of the passage were negligible. Boundary-
layer allowances of 0.005 inch per inch for the supersonic section and
0.01 inch per inch for the subsonic section were used in the design.
The pitch section of the 24-inch rotor passage designed to diffuse the
flow to a Mach number of approximately 0.55 is shown in figure 2.

2266

The compressor consisted of a rotor containing 53 blades and 23 inlet guide vanes. The rotor shown in figure 3 had a bulb type blade attachment, hub-tip radius ratio of 0.75, and pitch radius solidity of approximately 3.55.

APPARATUS

Compressor unit. - The installation for the 24-inch supersonic compressor rotor investigated was basically the same as that described in reference 4. The increased weight of the rotor necessitated a straddle mount bearing support instead of the cantilever mounting arrangement previously used (reference 4). A schematic drawing of the compressor unit is shown in figure 4.

The compressor rig was so designed that simple modification of the piping would permit operation either in Freon-12 or air. A closed loop system was used for the Freon-12 tests with the laboratory refrigeration system charging and purging the loop. Aircraft coolers installed in the exhaust lines were used to regulate the inlet stagnation temperature. The inlet stagnation pressure was manually controlled by a valve located in the return line of the laboratory refrigeration system.

Instrumentation. - The instrumentation used in this investigation was essentially the same as that described in reference 4. To determine air contamination while operating in Freon-12, a density balance device was used to check the Freon purity, which was maintained above 99 percent by volume. The compressor entrance nozzle, calibrated with a standard adjustable orifice by the method of reference 5, was used to measure the Freon-12 weight flow through the closed loop system. The accuracy of the weight flow determined by this method was approximately 1 percent.

PROCEDURE

Prior to the compressor investigation a complete study of the inlet-guide-vane performance was made with the compressor rotor removed. The guide-vane turning angle and exit mass-flow distribution were obtained at several entrance Mach numbers including choking conditions.

The compressor was operated over a range of nominal equivalent air-tip speeds from 1760 to 1184 feet per second in Freon-12. The peak-pressure-ratio point for each speed was obtained by closing the throttle until the audible stall condition was reached. The throttle was then opened a small increment and data were taken. To give the same relative rotor-entrance Mach number as in air the design tip speed in Freon-12 was calculated by a method similar to that given in reference 6. In

addition to the Freon investigation, a two-dimensional cascade investigation was made on the pitch section of the rotor blade passage using the same facilities and testing techniques as described in reference 7.

The rotor entrance conditions in Freon-12 were obtained from the weight-flow measurements and the mass flow and turning angle distribution observed in the guide-vane investigation. The entrance Mach numbers determined in this manner checked very closely with those obtained by using wall-tap data (fig. 5). The exit conditions were determined from survey instruments immediately behind the wheel. The weight-flow measurements obtained from the survey instruments were compared with the measurements from the calibrated entrance nozzle and agreed within 2 percent. The efficiency and total-pressure ratios were based on readings taken from thermocouple rakes and total-pressure probes in the entrance tank and downstream of the wheel.

The data obtained in Freon-12 were reduced by utilizing the charts of reference 8. When these charts were used to determine an average value of specific heat for the compression process, some error resulted in the computation of adiabatic efficiency. A trial computation of adiabatic efficiency was therefore made using the two available methods: the standard isentropic total-pressure - temperature relation method involving the average specific heats as determined from reference 8; and the enthalpy method using the Freon thermodynamic tables of reference 9. The efficiencies obtained by the two methods agreed within 2 percentage points. The adiabatic efficiency reported herein was calculated by the use of average specific heats. The value of specific heat used was an average of the stagnation value at the compressor inlet and exit. This method was probably as accurate as the use of Freon enthalpy tables requiring extrapolated values for the operating range of the compressor.

RESULTS

Over-all performance of compressor. - The performance map of the 24-inch supersonic compressor determined in Freon-12 and converted to equivalent results in air is shown in figure 6. At the equivalent tip speed of 1590 feet per second in air (approximately design tip speed) a maximum total-pressure ratio of 2.02 was determined at an adiabatic efficiency of 0.74 and a weight flow of 61.5 pounds per second. Because of the vertical weight-flow characteristic at design speed, supersonic inlet-passage flow conditions are assumed to exist over the entire annular height. The slope of the peak total-pressure ratio curve decreased as design speed was approached, and the compressor operating at 110 percent of design speed resulted in a slight increase in weight flow, but

2266

no further increase in pressure ratio. The performance of the compressor was characterized by a rapidly deteriorating flow process above design speed. This phenomenon is shown in the sharp drop-off in efficiency above design speed by the efficiency-weight flow plots of figure 6(b).

Entrance-flow distribution. - A comparison of the design and experimental relative entrance Mach number distributions as determined from the guide-vane investigation is shown in figure 7(a). The deviation of the experimental curve from the design was caused by induced guide-vane-turning effects as shown in figure 7(b) and explained in reference 10.

Distribution of flow at rotor exit. - The flow conditions behind the rotor were characterized by a substantial radial redistribution of the mass flow from tip to root. A comparison of the exit conditions with entrance and design conditions shown in figure 8 indicates the sharp gradients in mass flow, axial Mach number, and exit angle behind the wheel. The mass flow and axial Mach number distributions (figs. 8(a) and 8(b)) show that the boundary layer nearly fills the outer third of the passage. This condition could readily be associated with boundary-layer separation at the tip or separation along the blade that was centrifuged to the tip. In figures 8(b) and 8(c) the higher-than-design axial Mach number at exit and lower-than-design exit angle existing over the major portion of the passage indicate poor passage diffusion. A method of evaluating the diffusion in the free-stream portion of the flow using the discharge static pressure is shown in figure 9. This figure consists of a series of p_5/P_0 contours theoretically computed for assumed exit relative Mach numbers, based on the assumption that the total losses incurred by the flow equal the normal shock losses at the relative entrance Mach number. The experimental exit relative Mach number in the free stream at design conditions is then evaluated by plotting the experimental values of p_5/P_0 on this figure. The lowest subsonic Mach number to which the flow was diffused apparently is approximately 0.9.

Two-dimensional cascade performance. - A cascade investigation of the pitch section of the 24-inch supersonic-compressor rotor indicated a phenomenon similar to that described in reference 11; that is, the boundary layer thickens because of the presence of the shock and compresses a portion of the flow in front of the shock from the original value to a lower Mach number value. The boundary layer then continues to thicken and reaccelerates the free stream immediately behind the shock to a Mach number close to 1. A comparison of the design static-pressure distribution on the trailing surface of the blade with that obtained from experimental data (fig. 10) is qualitatively in agreement with the preceding explanation of the boundary-layer shock-interaction pattern. Instead of the sharp rise in pressure predicted from theory, the static-pressure rise through the shock was smooth. The boundary-layer shock-interaction pattern complicated the diffusion problem and resulted in a measured reduction of 27 percent in the effective passage area at the exit instead of the estimated 10 percent. Although figure 10 shows that

the predicted diffusion rate $\Delta(p_4/P_0)$ per inch of 0.05 was approximately maintained behind the shock, the increased boundary layer at the shock reduced the possible diffusion from a theoretical exit Mach number of 0.55 to an observed value of 0.8.

ANALYSIS OF RESULTS

The performance of the 24-inch supersonic-compressor rotor was very different from design because of the poor passage diffusion and the radial redistribution of the flow. Possible causes for this departure are: (1) the failure to establish conditions approaching simple radial equilibrium after the shock, (2) the effects of boundary-layer shock interaction overshadowing any theoretical approach·to simple radial equilibrium after the shock, or (3) a combination of both.

The problem of obtaining simple radial equilibrium behind the shock has been previously described as depending on the proper guide-vane performance and on obtaining the theoretical Mach number behind the shock. Calculations were therefore made to determine the relative effects of deviation in these conditions on the radial forces behind the shock. These effects are indicated in figure 11 where the unbalanced radial force is plotted as a function of radius. Shown in the figure are five curves of the unbalanced radial forces behind the shock for the following conditions: (1) design entrance conditions and the theoretical Mach number behind the shock for air, (2) design entrance conditions and the theoretical Mach number behind the shock for Freon-12, (3) design entrance conditions and a Mach number of 1.0 behind the shock for Freon-12, (4) experimental entrance conditions and a Mach number of 1.0 behind the shock for Freon-12, and (5) conditions existing in the 24-inch supersonic-compressor rotor of reference 2. In addition to the preceding five curves, the total pressure force behind the shock at experimental conditions (for condition (4)) is shown for comparison purposes. The maximum experimental deviation from design entrance Mach number (fig. 7(a)), which was due to guide-vane flow deviation, apparently produces a substantial departure from simple radial equilibrium or

$$\frac{d(p_4/P_0)}{d(r/r_t)} - \frac{(p_4/P_0)\ \gamma V_{\theta,4}^{\ 2}}{a_4^{\ 2}\ (r/r_t)} >> 0$$

While this effect is quite pronounced, figure 11 shows that obtaining a Mach number of 1.0 behind the shock instead of the theoretical Mach number results in a small unbalanced radial force F_r. This small force indicates that the unbalanced radial force behind the shock is markedly affected by the entrance-flow distribution and somewhat less affected by the deviation in assumed passage-flow conditions.

2266

The comparison of the theoretical radial forces in the present design with the theoretical radial forces in the 24-inch supersonic compressor of reference 2 (fig. 11) indicates that, even with the deviations, the present design theoretically reduced the radial forces through most of the passage as compared with the theoretical forces occurring in the 24-inch supersonic-compressor rotor of reference 2. The greatest reduction in radial force was obtained at the pitch where the entrance conditions are nearest design conditions. A smaller reduction is obtained at the root (radius, 9.0 in.) whereas at the tip where the deviation in entrance conditions is greatest, there is a higher unbalanced radial force than in the investigation of reference 2. This reduction in the theoretically computed radial forces over most of the passage did not result in improved passage flow.

The poor passage performance and the sharp radial redistribution of the mass flow towards the root may be the result of several combined effects: (1) the severe boundary-layer shock-interaction pattern at the tip, (2) radial forces resulting from failure to establish design entrance conditions, and (3) possible radial flow velocities in the supersonic region.

A severe boundary-layer shock-interaction pattern can be expected at the tip because of the larger growth in boundary layer at the tip than at the other radial sections. The following are the principal causes for this larger boundary-layer development: (1) the continuous outer shroud enables the accumulated boundary layer from the guide vanes to develop along the outer wall and (2) the centrifuging effects further aid the growth of the boundary layer at the tip region. The interaction of the normal shock with a thick boundary layer at the tip probably resulted in separation and severe radial-flow redistribution.

The boundary-layer problem in the supersonic compressor was two-fold in nature. The radial sections below the tip were confronted with a two-dimensional boundary-layer shock-interaction problem as indicated by the two-dimensional cascade study while the tip region experienced the aggravated effects of both boundary-layer accumulation and shock interaction. If, as the cascade investigation has indicated, a Mach number of 1.0 exists behind the normal shock, use of the Kantrowitz contraction ratio (reference 3) will set a minimum boundary-layer thickness after the shock because the available area as defined by the Kantrowitz contraction ratio is appreciably larger than that required by the flow at a Mach number of 1.0. If the Kantrowitz contraction ratio is exceeded, as outlined in reference 12, the boundary-layer growth along the blade surfaces would be decreased and the subsonic passage diffusion would thereby be improved. Alleviation of the boundary-layer shock-interaction problem at the tip could then possibly .be accomplished by bleeding off the low-momentum air at the tip.

SUMMARY OF RESULTS

The results of the investigation of the 24-inch shock-in-rotor type supersonic compressor designed for simple radial equilibrium behind the normal shock can be summarized as follows:

1. A maximum pressure ratio of 2.02 at an adiabatic efficiency of 0.74 and a weight flow of 61.5 pounds per second were obtained at an equivalent tip speed of 1590 feet per second.

2. The theoretical reduction of the computed radial forces over a large portion of the passage had no apparent effect on the redistribution of the flow for the rotor investigated. The boundary-layer shock-interaction pattern and other effects must be considered along with the theoretical computations of the radial forces.

3. Establishment of simple radial equilibrium behind the shock with entrance guide vanes presented a difficult problem since secondary flows made the required large gradient in guide-vane turning difficult to obtain experimentally at the rotor tip and root sections.

CONCLUSION

The following conclusion can be drawn from this investigation: The shock-in-rotor type supersonic compressor offers a serious problem in subsonic diffusion behind a normal shock which must be solved before good stage performance can be realized for this compressor type. Control of the shock-boundary-layer interaction would greatly reduce this problem.

Lewis Flight Propulsion Laboratory
    National Advisory Committee for Aeronautics
        Cleveland, Ohio.

REFERENCES

1. Wright, Linwood C., and Klapproth, John F.: Performance of Super-sonic Axial-Flow Compressors Based on One-Dimensional Analysis. NACA RM E8L10, 1949.

2. Johnsen, Irving A., Wright, Linwood C., and Hartmann, Melvin J.: Performance of 24-Inch Supersonic Axial-Flow Compressor in Air. II - Performance of Compressor Rotor at Equivalent Tip Speeds from 800 to 1765 Feet per Second. NACA RM E8C01, 1949.

3. Kantrowitz, Arthur, and Donaldson, Coleman duP.: Preliminary Investigation of Supersonic Diffusers. NACA ACR No. L5D20, 1945.

4. Ritter, William K., and Johnsen, Irving A.: Performance of 24-Inch Supersonic Axial-Flow Compressor in Air. I - Performance of Compressor Rotor at Design Speed of 1600 Feet per Second. NACA RM E7L10, 1948.

5. Ullman, Guy N., Hartmann, Melvin J., and Tysl, Edward R.: Experimental Investigation of a 16-Inch Impulse-Type Supersonic-Compressor Rotor. NACA RM E51G19, 1951.

6. Boxer, Emanual, and Erwin, John R.: Investigation of a Shrouded and an Unshrouded Axial-Flow Supersonic Compressor. NACA RM L50G05, 1950.

7. Wright, Linwood C.: Investigation to Determine Contraction Ratio for Supersonic-Compressor Rotor. NACA RM E7L23, 1948.

8. Huber, Paul W.: Use of Freon-12 as a Fluid for Aerodynamic Testing. NACA TN 1024, 1946.

9. Perry, John H.: Chemical Engineers' Handbook. McGraw-Hill Book Co., Inc. 2d ed., 1941, pp. 2577-2582.

10. Lieblein, Seymour, and Ackley, Richard H.: Secondary Flows in Annular Cascades and Effects on Flow in Inlet Guide Vanes. NACA RM E51G27, 1951.

11. Donaldson, Coleman duP.: Effects of Interaction between Normal Shock and Boundary Layer. NACA CB 4A27, 1944.

2266

12. Graham, Robert C., Klapproth, John F., and Barina, Frank J.: Investigation of Off-Design Performance of Shock-In-Rotor Type Supersonic Blading. NACA RM E51C22, 1951.
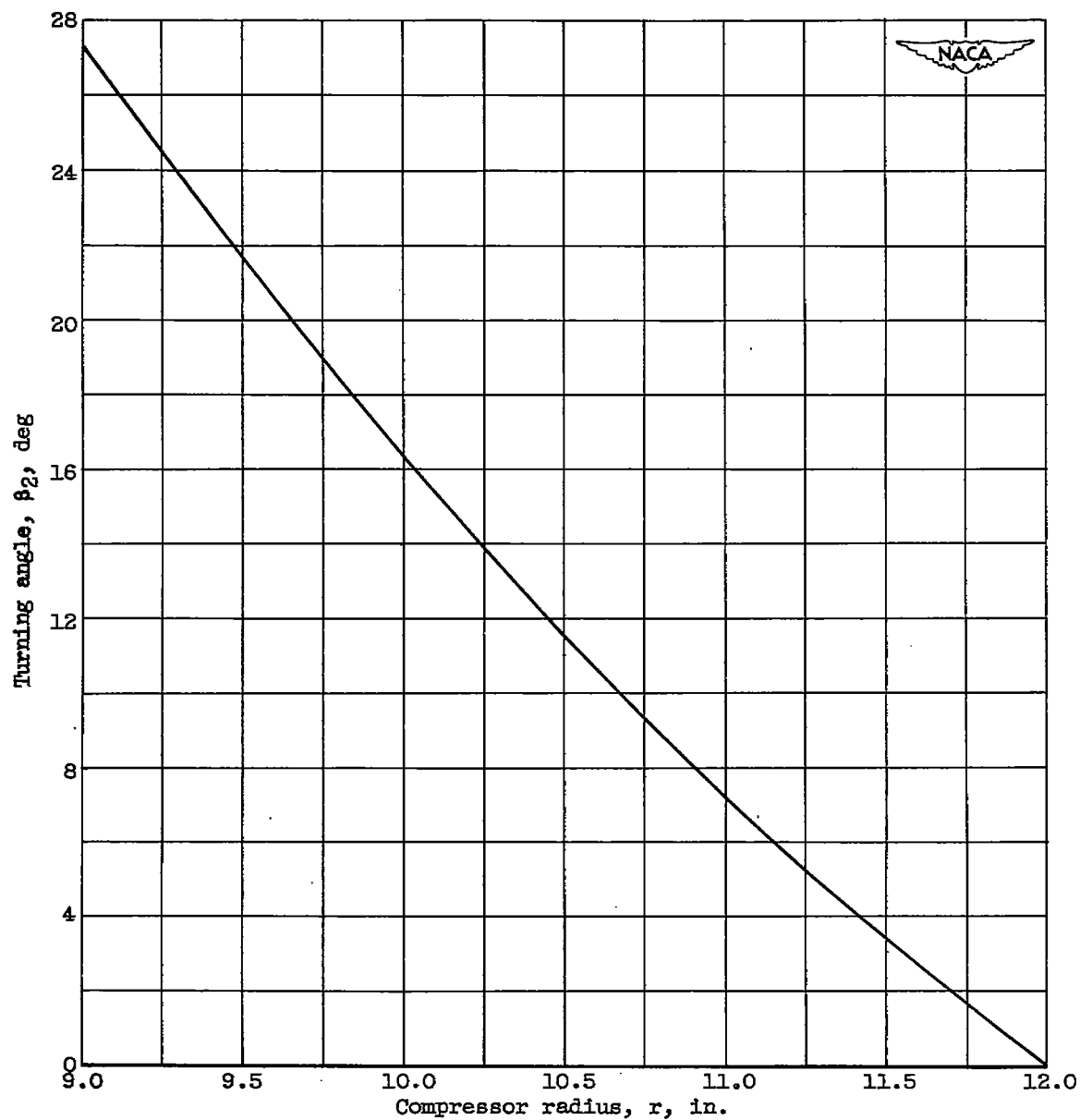
2266

2266

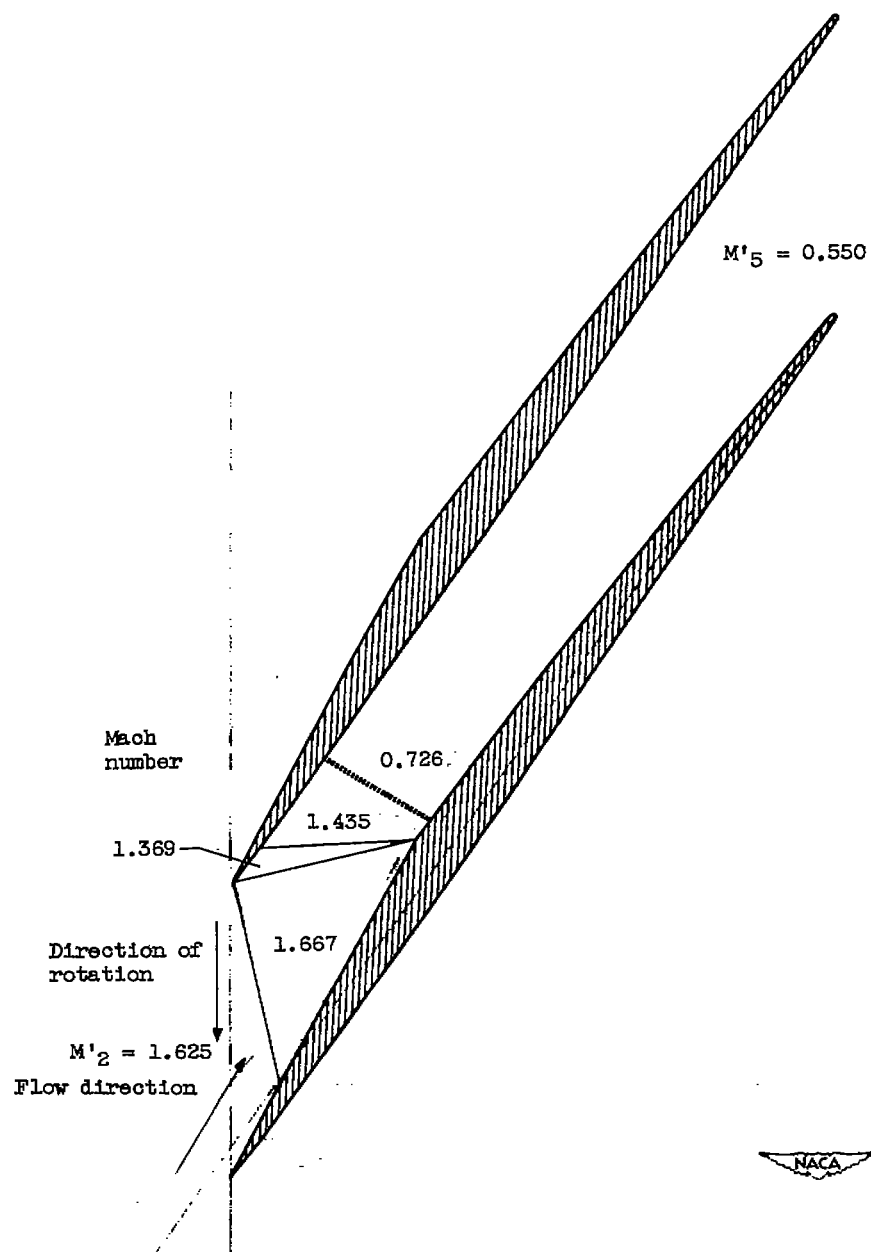Figure 1. - Design guide-vane turning distribution.

$M'_5 = 0.550$

Mach
number

0.726.

1.435

1.369

1.667

Direction of
rotation

$M'_2 = 1.625$
Flow direction

NACA

Figure 2. - Design pitch section of 24-inch supersonic-compressor rotor.
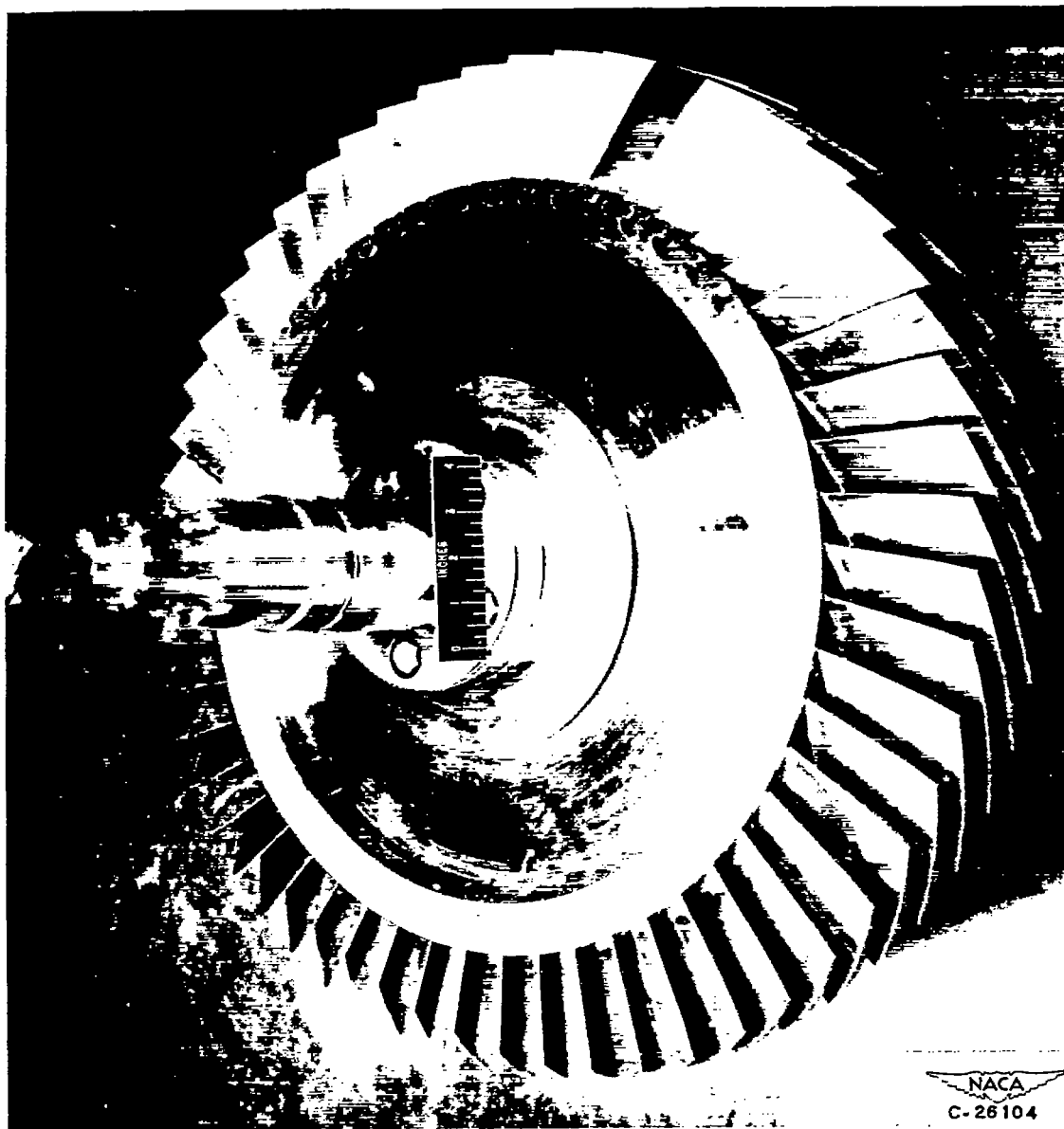
Figure 3. - 24-Inch supersonic compressor rotor.

Entrance tank

Survey
instrument

Total-
pressure
rake

Discharge
throttle

Rotor

Guide
vane

Bearing

Entrance
nozzle

NACA
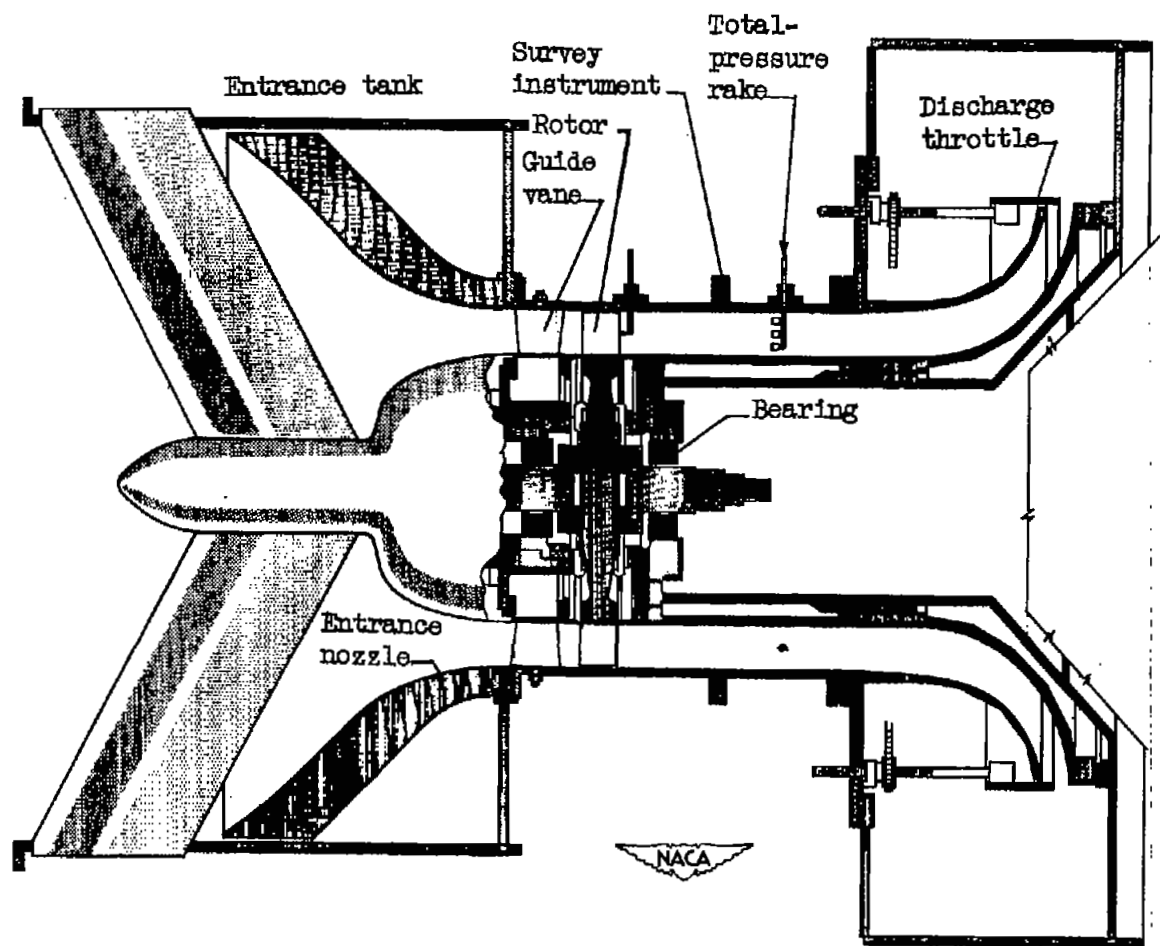
Figure 4. - Compressor unit.

2266

2266
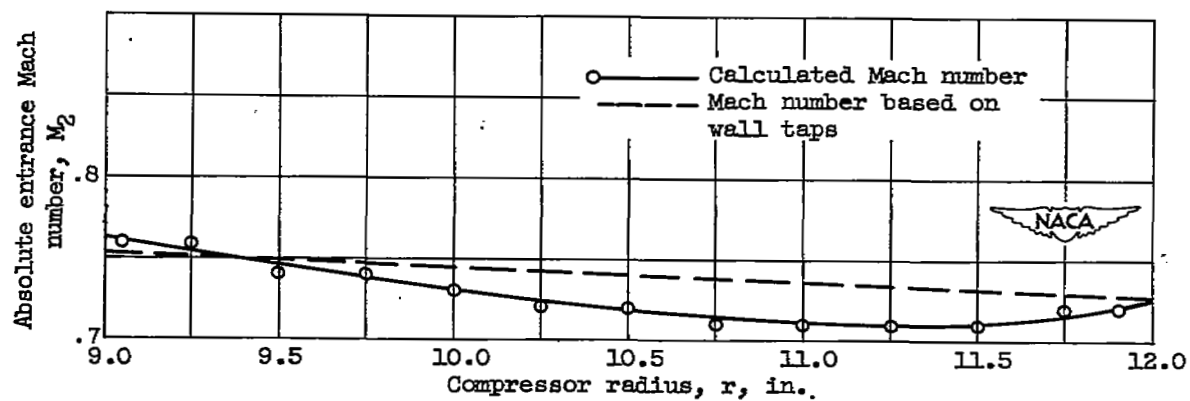
Figure 5. - Comparison of calculated absolute entrance Mach number
distribution with Mach number based on wall-tap data.
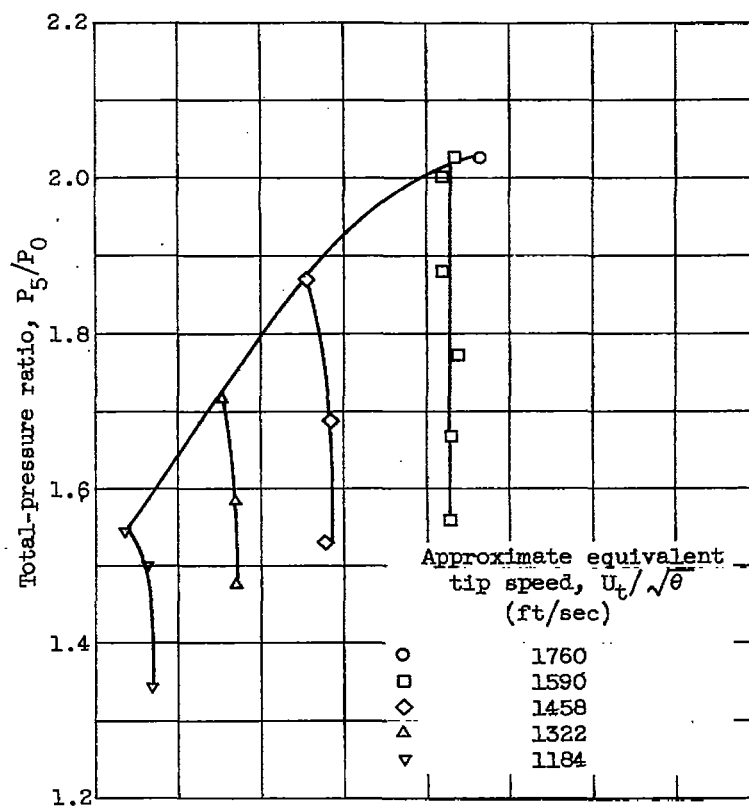
(a) Total-pressure ratio; measured in Freon-12.
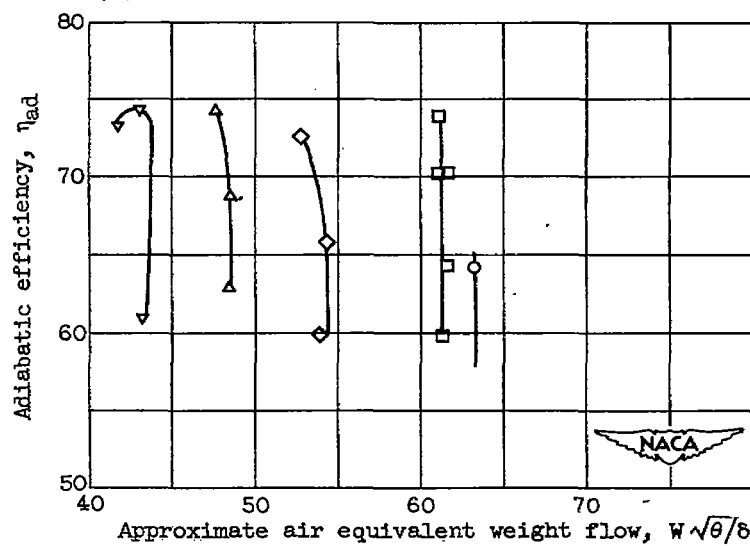
(b) Adiabatic efficiency; measured in Freon-12.

Figure 6. - Performance characteristics of 24-inch
supersonic-compressor rotor.
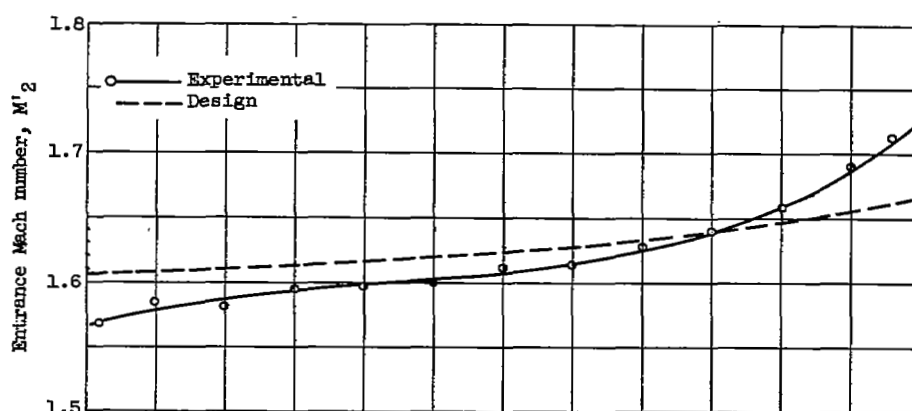
(a) Relative entrance Mach number distribution.
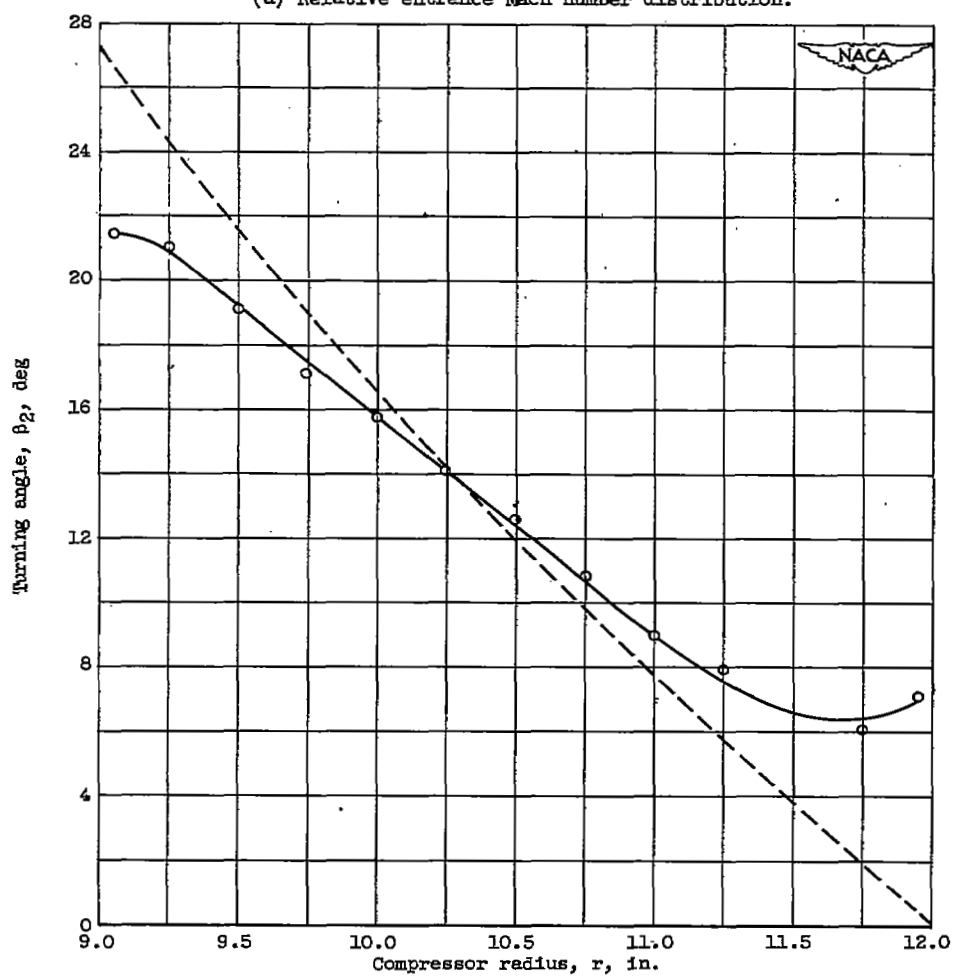
(b) Guide-vane turning.

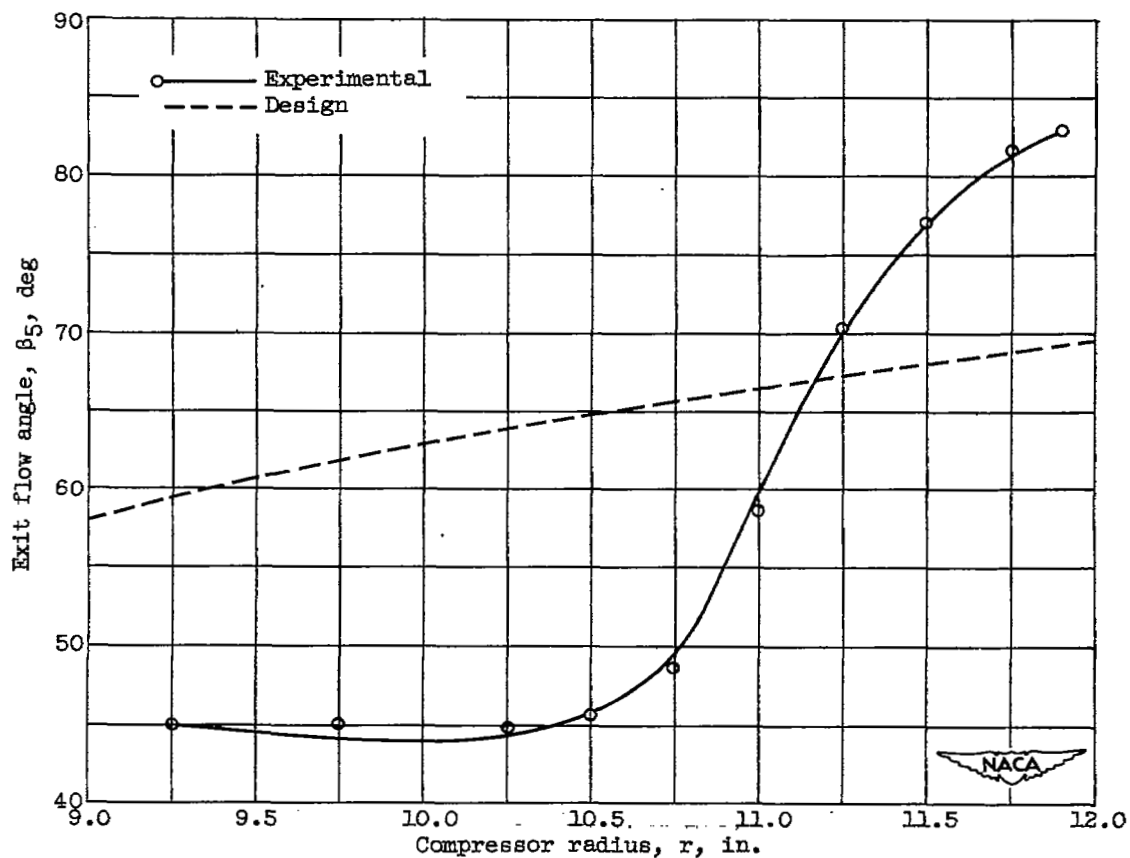Figure 7. - Rotor entrance conditions; design tip speed (1600 ft/sec).
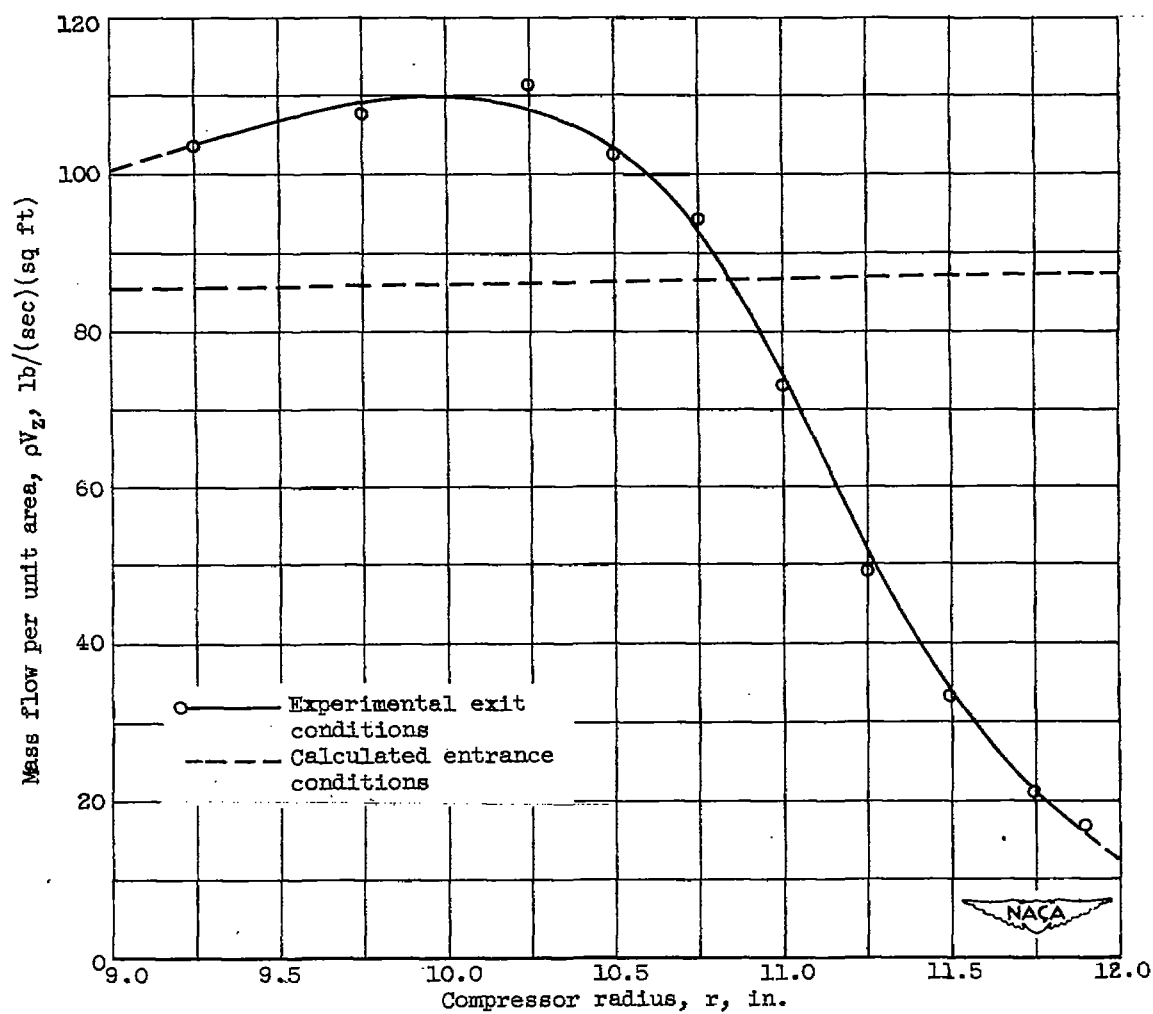
(a) Mass flow distribution.

Figure 8. - Comparisons of rotor exit conditions with entrance
and design conditions; measured in Freon-12.

2266
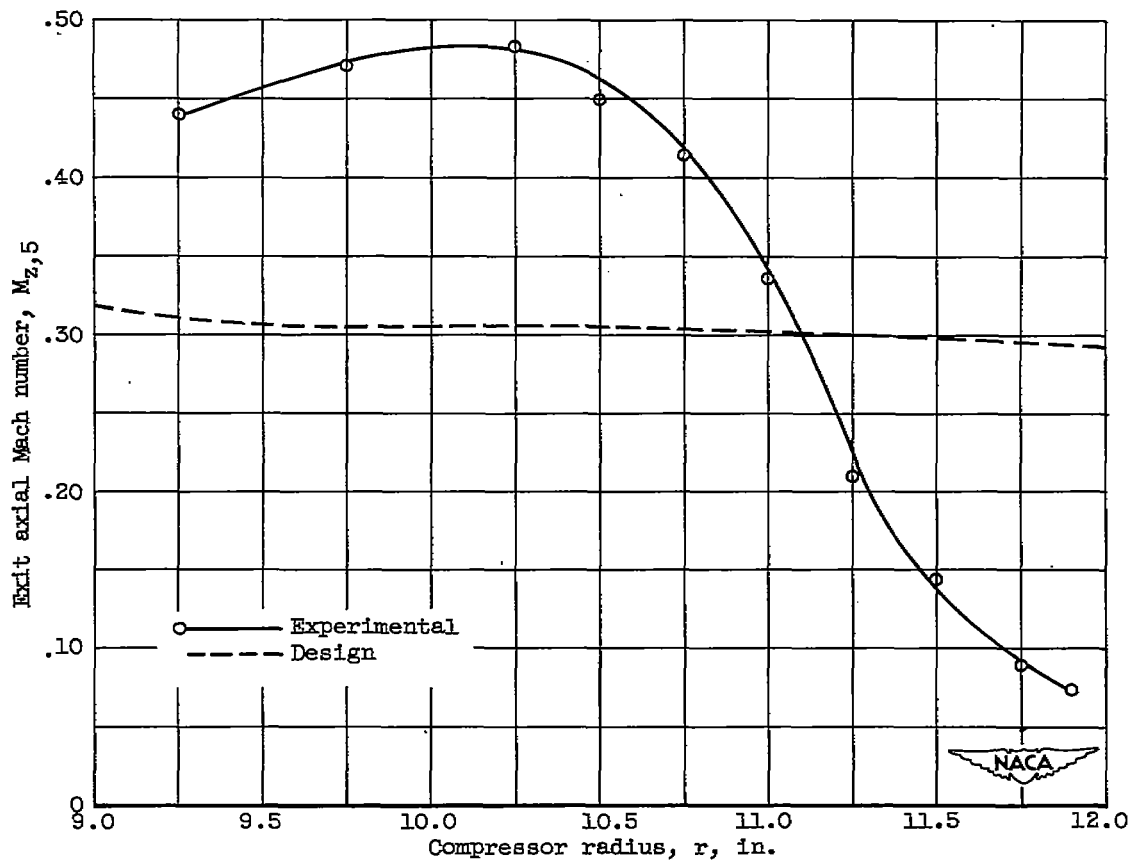
(b) Axial Mach number distribution.

Figure 8. - Continued. Comparisons of rotor exit conditions with
entrance and design conditions; measured in Freon-12.

(c) Exit angle distribution.

Figure 8. - Concluded. Comparisons of rotor exit conditions with
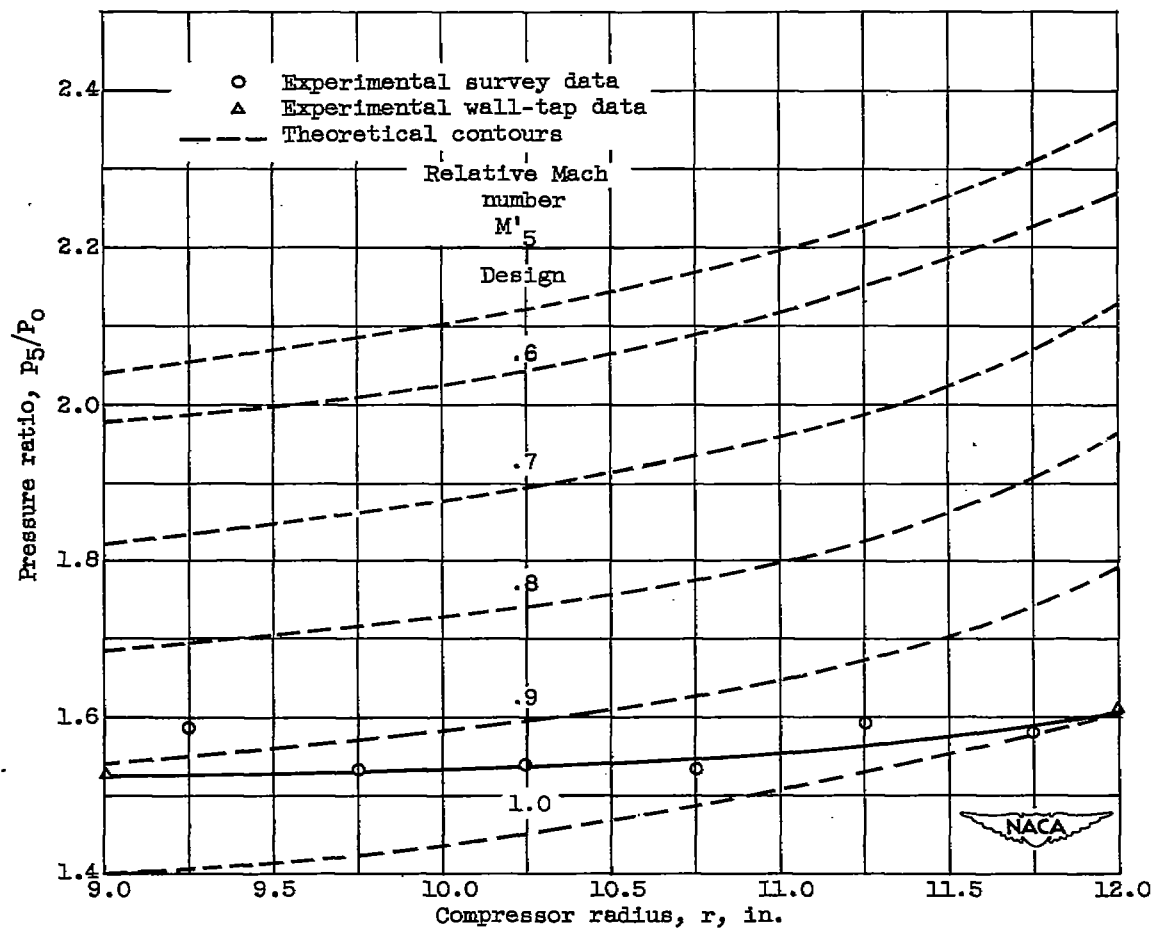entrance and design conditions; measured in Freon-12.

Figure 9. - Comparison of experimental and theoretical static-
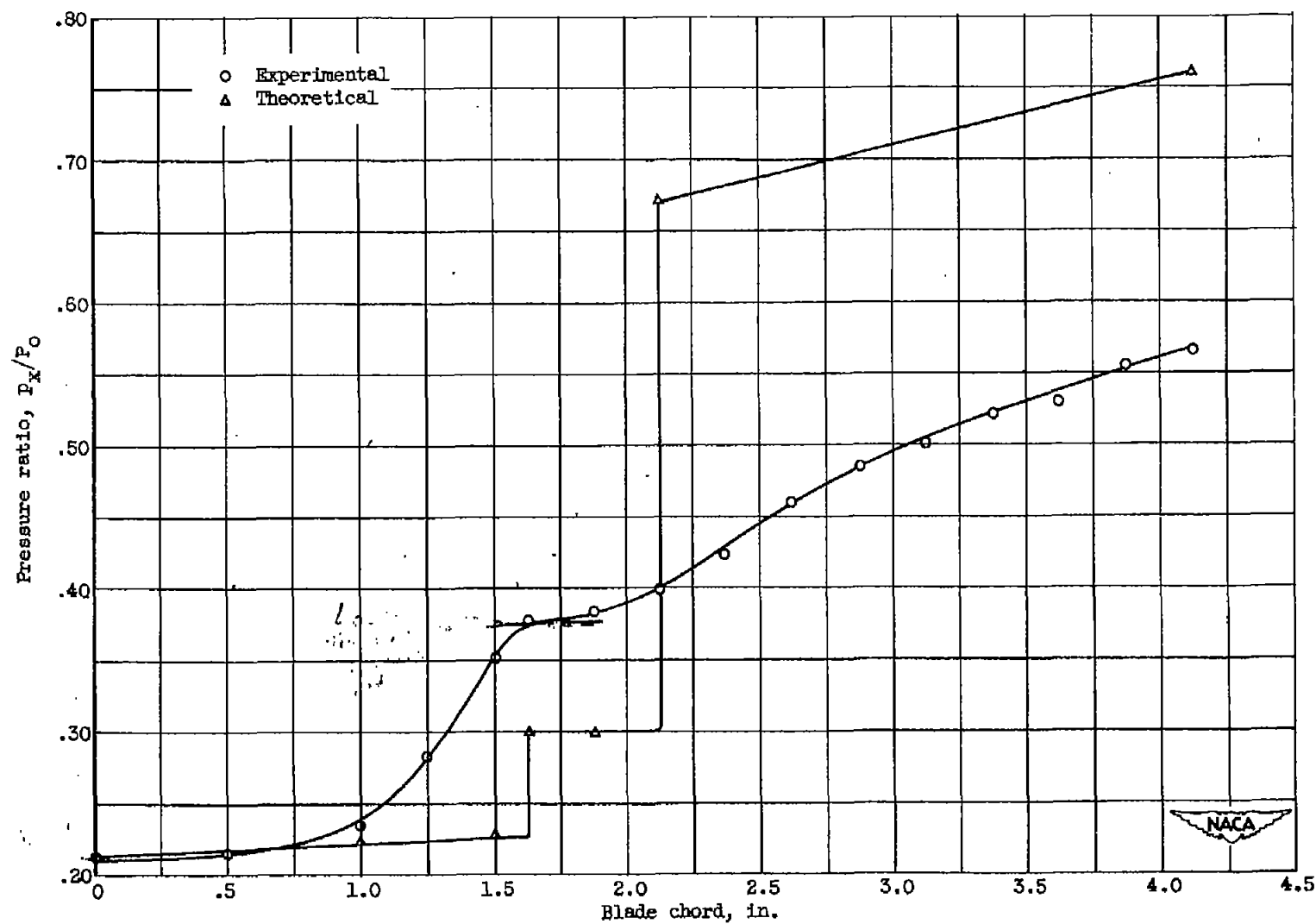pressure distribution at rotor exit.

Figure 10. - Comparison of theoretical and cascade static-pressure distribution on trailing surface of blade.
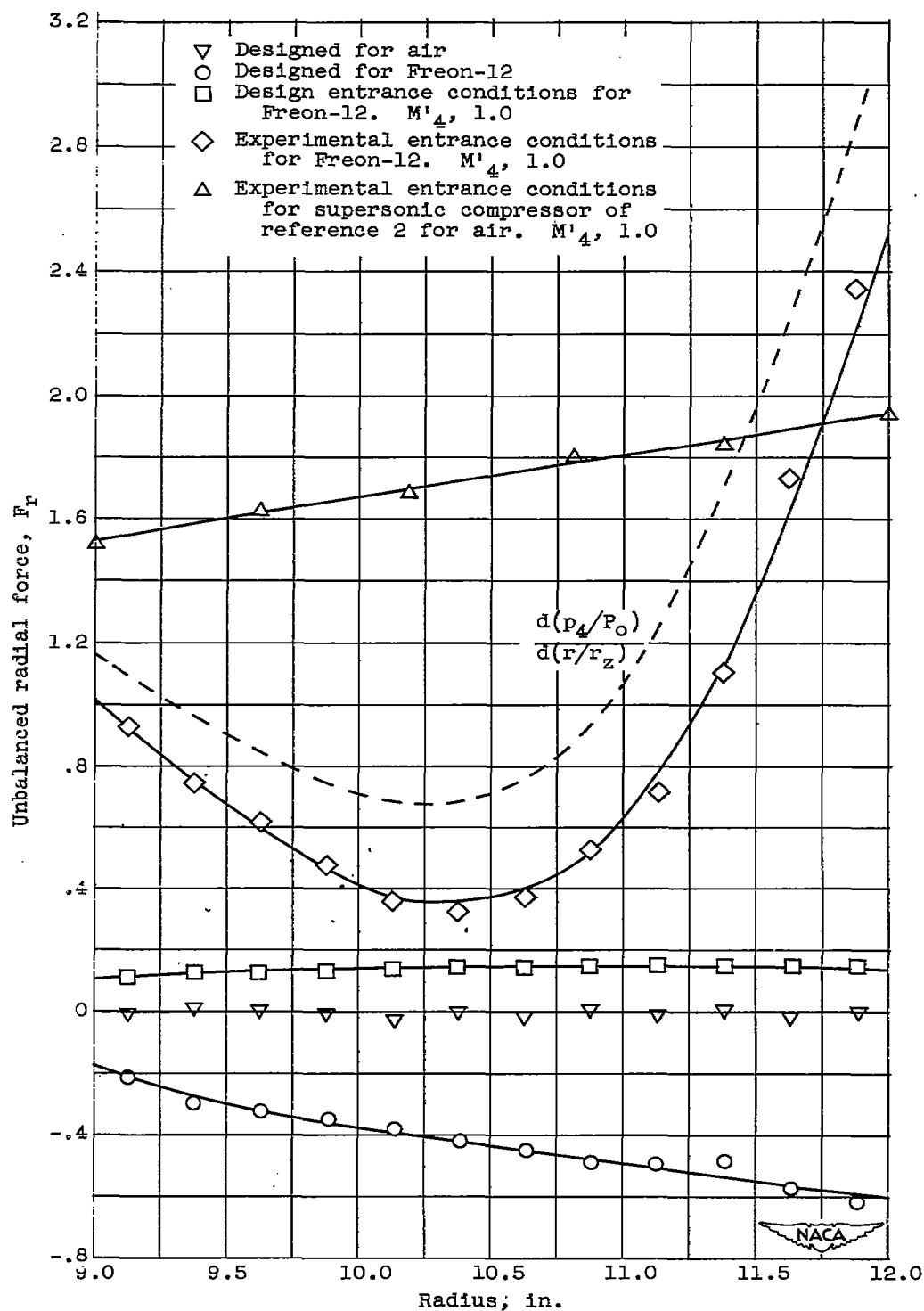
Figure 11. - Variation of unbalanced radial force behind normal
shock.